

Verification of Breast Cancer Treatment Planning with Various Radiation Techniques Using Monte Carlo Simulations and Linac Log Files

R. D. Sugandi^{1,2}, A. Azzi¹, M. Fadli³, D. S. K. Sihono^{1*}

¹Department of Physics, Faculty of Mathematics and Natural Sciences, Universitas Indonesia, Depok, 16424, Indonesia

²Installation of Radiology, Unit Radiotherapy, Pertamina Central Hospital, Jakarta, 1383, Indonesia

³Department of Radiation Oncology, Mochtar Riady Comprehensive Cancer Center, Jakarta, 12930, Indonesia

ARTICLE INFO

Article history:

Received 23 January 2025

Received in revised form 21 April 2025

Accepted 12 June 2025

Keywords:

Dynalog files

Monte Carlo

Patient-specific quality assurance

Radiotherapy

ABSTRACT

Due to the complexity of radiotherapy techniques, rigorous Patient-Specific Quality Assurance (PSQA) is crucial to ensure the accuracy of treatment plans. This study aims to evaluate the performance of the Treatment Planning System (TPS) by comparing its dose distribution calculations with those obtained from the PRIMO Monte Carlo simulation. Treatment plans for 3D-CRT, IMRT, and VMAT were generated for a Rando breast phantom using the TPS. Subsequently, the dose distributions from the TPS were compared with those obtained from the PRIMO Monte Carlo simulation. Key metrics, including Homogeneity Index (HI) and Conformity Index (CI), were calculated to assess the quality of dose distribution. Furthermore, the dose constraints on OARs were evaluated to assess the impact on surrounding healthy tissues. To further validate the TPS, dose distributions from the linac log file (Dynalog) for VMAT were reconstructed within the PRIMO environment. These reconstructed distributions were then compared with the dose distributions calculated directly by the TPS. Gamma index analysis was employed to evaluate the agreement between these two sets of data. The comparison between TPS and Monte Carlo simulations revealed that 3D-CRT plans exhibited smaller deviations in HI and CI compared to IMRT and VMAT plans. However, a significant improvement in HI and CI values was observed in both IMRT planning simulations and Dynalog VMAT file simulations, indicating enhanced plan quality. The dose received by OARs in all treatment plans remained within the acceptable dose thresholds, demonstrating effective sparing of surrounding healthy tissues. For the PSQA procedure, the 3D-CRT technique is still the safest due to its lower level of complexity compared to IMRT and VMAT. More complex treatments should consider the robustness of treatment transfer information from TPS to linac to avoid dosimetry errors.

© 2025 Atom Indonesia. All rights reserved

INTRODUCTION

Radiation therapy is one of the main methods in breast cancer treatment, which aims to destroy cancer cells while minimizing damage to surrounding healthy tissue. Among the various techniques available, Intensity Modulated Radiotherapy (IMRT), and Volumetric Modulated Arc Therapy (VMAT) are modern approaches that have been widely used. Both techniques offer high flexibility and precision in delivering radiation

doses that are appropriate to the shape and position of the tumor, especially in cases of breast cancer that often has a complex anatomical distribution.

The advantages of IMRT and VMAT lie in the ability to set complex parameters, such as multi-leaf collimator (MLC), radiation beam fluence, and configuration on the linear accelerator (linac) head. However, the complexity of this dosimetry planning requires an automated algorithm capable of generating optimal parameters to ensure maximum dose to the tumor without harming the surrounding healthy tissue [1]. As a consequence of the high level of precision, a strict Quality Assurance (QA) procedure is required, especially

*Corresponding author.

E-mail address: dwi.seno@sci.ui.ac.id

DOI:

39through the Patient Specific Quality Assurance
40(PSQA) approach, to ensure the accuracy of the dose
41distribution according to the planning.

42 PSQA plays an important role in ensuring the
43concordance between planning and therapy delivery,
44especially in cases requiring adaptive radiotherapy
45(ART), which is the process of adapting planning
46due to changes in patient anatomy during the course
47of therapy [2]. The PSQA procedure is usually
48performed based on guidelines from the American
49Association of Physicists in Medicine (AAPM) Task
50Group No. 218, which recommends tolerance
51criteria, such as gamma pass rate (GPR) $\geq 95\%$ with
52dose difference (DD) and distance to agreement
53(DTA) criteria parameters of 3%/2 mm and a dose
54threshold of 10 % [3].

55 To improve the efficiency and accuracy of
56PSQA, Monte Carlo simulation-based software,
57such as PRIMO, has been widely used. PRIMO
58is able to simulate dose distribution precisely, which
59is useful for evaluating modern radiotherapy
60planning. Several studies, such as those conducted
61by Aamri et al. (2021) and Altuwayrish et al. (2022),
62showed that PRIMO simulation results are
63comparable to other TPS systems, with dose
64distributions still within clinical tolerance limits
65[4,5]. In addition, PRIMO can also utilize Varian's
66linac log file called dynalog to analyze the dynamic
67movement of the device, including the MLC,
68which contributes to the evaluation of the suitability
69of therapy planning and implementation [1].

70 In addition, the accuracy standards
71recommended by AAPM, such as the root-mean-
72square error (RMS) limit of 3.5 mm [6],
73are considered too loose for certain clinical
74applications. Some researchers suggest a tighter
75RMS limit of from 3.3 to 1.0 mm to improve the
76reliability of modern radiotherapy systems [7,8].
77Therefore, re-evaluation of dosimetry parameters
78using stricter standards is needed to ensure the
79safety and effectiveness of radiation therapy,
80especially in breast cancer.

81 This study aims to reconstruct the planning and
82verify the dose distribution using PRIMO software on
833D-CRT, IMRT, and VMAT techniques for breast
84cancer therapy. In addition, this study also evaluates
85the dose distribution on PRIMO with dynalog linac
86input to determine the accuracy of the information
87transfer made by the TPS to the linac machine.

88

89

90 **METHODOLOGY**

91 **Treatment planning**

92 Female Alderson RANDO Phantom
93(RSD inc, Canada) was utilized to simulate a left
94whole breast cancer irradiation. The phantom was
95planned to be exposed with a Varian iX linac with a

96 MV photon beam. Three techniques, i.e.,
973D Conformal Radiation Therapy (3DCRT), IMRT,
98and VMAT, were used to obtain the dose distribution
99and the transfer information differences between
100different complexity plans. Prescribe dose was
1015000 cGy to the mean dose for IMRT and VMAT and
102to the isocenter for 3DCRT. For 3DCRT, two radiation
103fields were performed with the Field in Field
104technique. For the IMRT and VMAT, seven radiation
105fields and two arcs were performed, respectively.
106MLC and Jaws positions were generated manually for
1073DCRT, and automatically for IMRT and VMAT
108using the optimization algorithm.

109 All the plans were calculated by using Eclipse
110ver.13.6 (Varian, Canada) and an analytical
111anisotropic algorithm (AAA). After the treatment
112plan was approved. The treatment information,
113such as CT images, structures, plans, and doses,
114was exported to DICOM format.

115

116

117 **Dynalog file**

118 The treatment plans were transferred to the
119linac's console for one fraction of 200 cGy in QA
120mode. To obtain the dynalog file, automatic storage on
121the linac console needs to be activated. Then, the linac
122performs irradiation for three variations of techniques.
123After that, the folder containing the planning data and
124the dynalog files in ".dlg" format is copied for the
125Monte Carlo simulation.

126

127

128 **Monte carlo simulation**

129 The Monte Carlo simulation consists of three
130parts. First, the commissioning of the Monte Carlo
131to the baseline data of the linac. Second,
132the simulation of the female RANDO phantom by
133using the RT-plan input. Third, the simulation of the
134same phantom with the log-file input.

135 The commissioning part began with tuning the
136initial parameters of PRIMO Monte Carlo. The
137following parameters were: Initial energy: 6.2 MeV,
138Energy FWHM: 0.186 MeV, Focal spot FWHM:
1390.15 cm, Beam divergence: 2.5 degrees

140 These parameters are in accordance with the
141research conducted by Rodriguez [1]. Considering
142that each linac is unique, the output of the Monte
143Carlo simulation at the initial parameters is adjusted
144to the radiation output of the Varian iX linac at our
145hospital. In this research, the simulation was divided
146into two segments. The first segment was the fixed
147component of the gantry, and the second one was the
148beam parameter and phantom. The simulation was
149performed using 10^8 particle histories in the first
150segment. The results in this segment can be used as
151input in the second segment.

152 Monte carlo simulation on RANDO phantom

153 Simulations on the RANDO phantom
 154 were divided into 2, i.e. based on the radiotherapy
 155 plan (RT-plan) and based on the dynalog after
 156 irradiation. Monte Carlo simulations on the
 157 RANDO phantom were in the second segment
 158 which combine the moving linac parameters like
 159 gantry angle, jaws, mlc position and phantom
 160 information. Simulations are carried out with
 161 10^8 particle histories and applying a coarse dose
 162 distribution to speed up the simulation time.
 163 Besides, the simulation applied variance reduction
 164 technique of splitting factor of 300 to boost
 165 the computation time. Simulations were carried
 166 out for each RT-plan and dynalog files, so that each
 167 produces a dose distribution.

168

169

170 Evaluation and analysis

171 The quality of plan and simulation were
 172 evaluated by using the Homogeneity Index (HI) and
 173 Conformity Index (CI) for the target volume. For
 174 OARs, the evaluation followed the dose constraints
 175 for each organ. In this study, the 5 OARs selected
 176 based on the highest priority level such as Ipsilateral
 177 Lung, Contralateral Lung, Heart, and Spinal Cord
 178 [9]. To find the HI value, the Eq. (1) recommended
 179 by ICRU 83 was used.

180

$$HI = \frac{D_{2\%} - D_{98\%}}{D_{50\%}} \quad (1)$$

181

182 When HI values approaching zero indicate high
 183 uniformity of dose distribution in the target volume
 184 [10]. Meanwhile, CI values can be obtained from the
 185 following Eq. (2).

186

$$CI = \frac{Vol_{95\% Coverage}}{Vol_{PTV}} \quad (2)$$

187

188 where $Vol_{95\% coverage}$ is the total volume that
 189 receives 95 % of the prescription dose, Vol_{PTV} is
 190 the target volume. A value of 1 in the CI represents
 191 complete coverage of the prescription dose in
 192 the target volume without affecting the
 193 surrounding tissue [11].

194 In addition, gamma index analysis was
 195 performed by comparing the planned dose
 196 distribution with the Monte Carlo simulation Monte
 197 Carlo simulation was used as a reference in this
 198 comparison [12]. The dose distribution evaluation
 199 included global gamma pass rate (GPR) values with
 200 3%/3mm criteria and 10 % dose threshold by using
 201 the built-in algorithm from PRIMO. The overall
 202 research was described in Fig. 1.

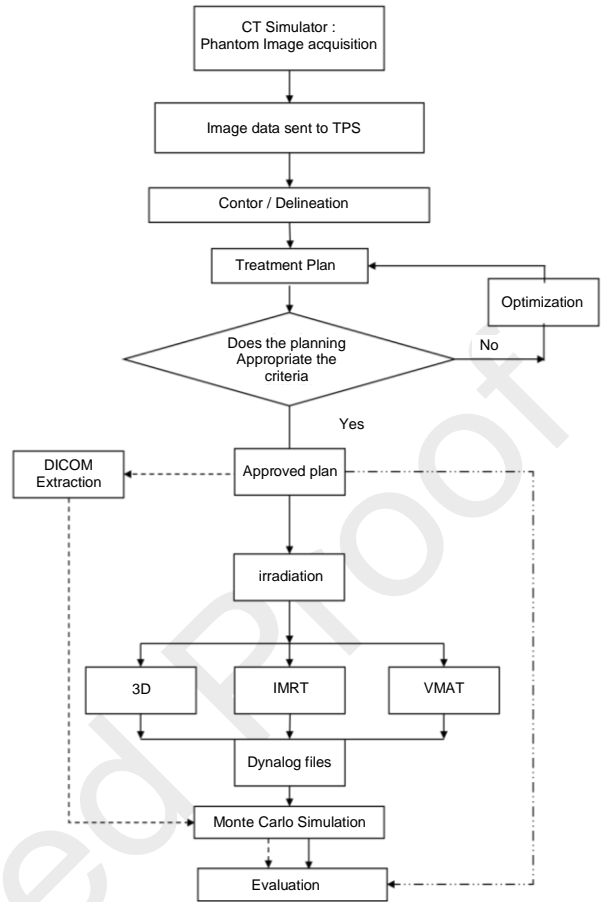
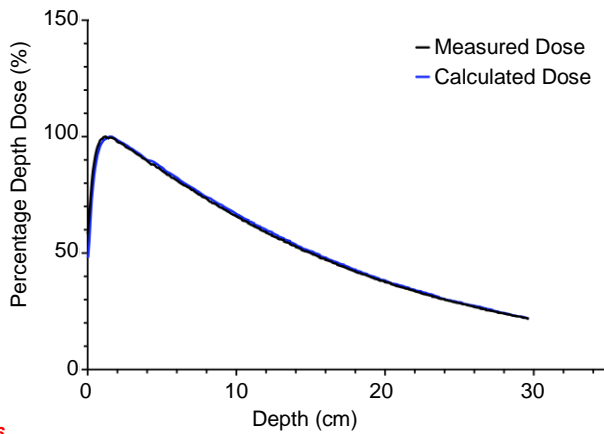


Fig. 1. Research flow diagram. The solid line represents the treatment plan and dynalog file input for Monte Carlo simulation. The dash line represents the Monte Carlo simulation with radiotherapy plan as input. The dash and dot line means the approved dose distribution to evaluate with both Monte Carlo simulation.

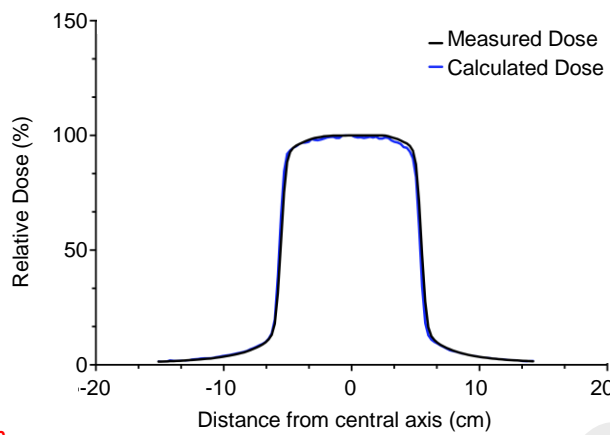
206 RESULTS

207 Monte carlo validation

208 The differences in PDD and beam profile
 209 between simulation and measurement results
 210 can be seen in Fig. 2. The blue line was the result of
 211 the Monte Carlo simulation calculation, while the
 212 black line was the baseline data. Visually, their
 213 differences were shown at the edge of the
 214 beam profile. This could be happened because
 215 of the fluctuation of particle deposition on
 216 Monte Carlo. The uncertainty of Monte Carlo
 217 simulation for this section was 1.4 %. Thus, the
 218 statistical of the Monte Carlo was quite good.
 219 The GPR of the PDD and beam profile were 99.8 %
 220 and 99.2 % for criteria of 2%/2mm, respectively.
 221 In addition, validation is carried out according
 222 to the IAEA TRS-430 procedure by comparing
 223 the confidence limits in several areas on the
 224 PDD and the beam profile. The results are shown
 225 in Table 1.



(a)



(b)

Fig. 2. (a) PDD and (b) beam profile of simulations in PRIMO (blue) and baseline data (black) at $10 \times 10 \text{ cm}^2$ and 10 depths for the beam profile.

Table 1. Evaluation points on PDD and beam profile for a $10 \times 10 \text{ cm}^2$ field at a depth of 10 cm

Properties	Area	Evaluation	Tolerance Limit
PDD	δ_1	2.2 %	2 %
	δ_2	1.3 mm	2 mm
	δ_2	0.2 mm	2 mm
Beam Profile	δ_3	1.8 %	3 %
	δ_4	10.4 %	30 %
	δ_{50-90}	0.2 mm	2 mm
	RW ₅₀	0.03 mm	2 mm

simulation result unit is in eV/g while the desired dose has a unit of Gy. Based on the reference measurement on the linac, the measurement dose rate value is 0.943 cGy/MU at a depth of 10 cm with a field size of $10 \times 10 \text{ cm}^2$. While the output value of the Monte Carlo simulation is 0.8 eV/g. Therefore, the calibration factor of the Monte Carlo simulation reference dose estimate is 1.2 cGy/MU g/eV.

252

253

254 Monte carlo evaluation on RANDO 255 phantom

To generate dose distributions, each patient's planning data was simulated individually. These patient-dependent segments require approximately 3 hours for each treatment. Dosimetry evaluation was conducted to determine the distribution of doses in the tissue exposed to radiation. For PTV, HI and CI were used as the evaluation metrics. On the other hand, dose constraints recommended by Radiation Therapy Oncology Group (RTOG) was employed for OAR evaluation.

The HI and CI of this study can be seen in Table 2. The HI value approaching zero indicates better dose coverage in the target volume, and the CI value approaching one indicates prescription dose coverage in the target volume by minimizing OAR exposure. In the TPS, the 3DCRT technique produces a relatively high HI value (0.2), which was possible that most of the dose was distributed in the periphery of the target due to parallel opposing technique. In the IMRT technique produced excellent HI values (0.1), indicating a more uniform dose distribution to the target. VMAT showed HI equal to IMRT. Furthermore, both RT-plans and dynalog files were imported to PRIMO Monte Carlo and showed that the HI for 3DCRT remains constant rather with deviation of 0.02 than IMRT and VMAT where the deviation were 0.1 and 0.3, respectively.

The CI value for the CI parameter in all techniques was generally high (≥ 0.95), except for the VMAT technique (0.68). The difference in CI values between 3DCRT and IMRT techniques for CI parameters was 0.02. This indicates that both techniques have almost the same level of accuracy when it comes to achieving the coverage distribution on the target. Similar to HI, the smallest deviation of CI when compared to MC simulation was found on 3DCRT with a standard deviation of 0.01, while the IMRT and VMAT were 0.1 and 0.1. Additional dose statistics for PTV were deficit in Table 2.

226
227
228
229

230
231
232
233

234
235

236

From the evaluation conducted, the simulation parameters for the 6 MV photon beam on PRIMO matched the radiation output of the 6 MV photon radiation of the Varian iX linac at our hospital. To obtain the absolute dose in the Monte Carlo simulation, a calibration value was needed between the Monte Carlo results and the baseline. This is because the

Table 2. Comparison of dose evaluation parameters on PTV for three technique variations (3DCRT, IMRT, VMAT) and three calculation methods (TPS, MC, MC Log).

Or-gan	Para-meter Dosis	3D CRT			IMRT			VMAT		
		TPS	MC	MC Log	TPS	MC	MC Log	TPS	MC	MC Log
PTV	HI	0.2	0.2	0.2	0.1	0.4	0.2	0.1	0.2	0.8
	CI	1.0	0.9	0.9	1.0	0.8	1.0	1.0	0.9	0.7
	Dmean (Gy)	5130	50.7	50.7	55.5	51.6	51.8	59.5	50.8	54.4
	D2 (Gy)	5306.6	5348.1	5347.9	5333.6	6181.1	5521.2	5354.2	5418.6	7688.8
	D98 (Gy)	4495.0	4325.3	4325.9	4921.7	4159.6	4691.6	4619.5	4319.5	3255.0
	V90 (%)	97.9	96.5	96.6	99.9	91.9	99.0	96.1	96.6	74.5
	V95(%)	94.9	92.8	92.8	99.6	81.1	97.4	95.0	92.1	67.8

298*MC = Monte Carlo simulation with input from RT-plan

299MC Log = Monte Carlo simulation with dynalog input

300

301

302 **Organ at risk evaluation**

303

Table 3. Comparison of dose evaluation parameters on various OARs for three techniques variations (3DCRT, IMRT, VMAT) and three calculation methods (TPS, MC, MC Log).

OAR	Dose Parameters	3D CRT			IMRT			VMAT		
		TPS	MC	MC Log	TPS	MC	MC Log	TPS	MC	MC Log
Total Lungs	D _{mean} (Gy)	1.1	1.2	1.2	7.7	3.6	7.9	4.0	4.2	3.7
	V ₅ (%)	3.3	3.3	3.3	57.3	17.2	58.4	22.5	23.4	18.4
	V ₁₀ (%)	1.8	2.1	2.1	27.8	16.9	28.9	9.1	9.9	8.2
Lung Ipsi	D _{mean} (Gy)	2.3	2.4	2.4	10.9	7.1	11.0	5.9	6.1	5.8
	V ₅ (%)	7.2	7.2	7.2	64.8	32.3	65.1	32.4	32.4	30.8
	V ₁₀ (%)	3.9	4.6	4.6	52.6	32.2	52.5	19.1	20.1	17.9
	V ₂₀ (%)	2.4	3.0	3.0	15.1	16.5	15.9	7.1	7.9	7.3
	V ₃₀ (%)	1.7	2.3	2.3	3.2	4.7	4.2	2.3	3.1	2.9
Lung Contra	D _{mean} (Gy)	0.1	0.3	0.3	5.1	0.6	5.3	2.5	2.6	1.9
	V ₅ (%)	0.0	0.0	0.0	50.9	4.4	52.7	14.3	15.9	7.9
	V ₁₀ (%)	0.0	0.0	0.0	7.2	4.1	8.9	0.7	1.36	0.0
Breast Cons	D _{mean} (Gy)	0.9	1.6	1.6	6.2	2.4	6.7	6.8	7.3	5.5
	D ₁ (Gy)	18.5	27.6	27.6	19.8	24.2	23.9	20.3	22.3	17.5
Heart	D _{mean} (Gy)	1.3	1.2	1.2	14.4	12.0	14.4	6.9	6.9	7.4
	V ₅ (%)	0.9	1.2	1.3	100.0	74.8	100.0	59.2	58.4	67.8
	V ₁₀ (%)	0.3	0.5	0.5	92.8	74.4	93.3	21.8	21.5	25.1
	V ₂₅ (%)	0.0	0.1	0.1	1.1	2.1	1.2	0.1	0.3	0.0
Spinal cord	D ₁ (Gy)	0.3	0.3	0.3	9.2	10.7	9.0	2.2	2.3	2.4

304

305

306 This study focuses on the analysis of the 318 on the MC with dynalog input, which reflects a 307 average dose, low and high dose distribution, 319 greater dose exposure on the target side. In contrast, 308 and other critical parameters on vital organs such as 320 the 3DCRT technique with TPS shows the lowest 309 the lungs, heart, and spinal cord. The evaluation 321 D_{mean} of 2.3 Gy, which indicates better protection for 310 results are summarized in detail in Table 3. 322 OARs on the ipsilateral side. The exposed dose to 311 The mean dose (D_{mean}) for the total lung 323 the contralateral lung was consistently lower than 312 showed significant variation between techniques 324 the ipsilateral. The IMRT technique with MC Log 313 and calculation methods. The IMRT technique with 325 recorded the highest D_{mean} value of 5.2 Gy, while the 314 the MC Log method produced the highest D_{mean} of 326 3DCRT technique gave a lower value, approaching 315 7.9 Gy, while the 3DCRT technique with TPS 327 zero. This suggested that IMRT, although more 316 recorded the lowest value of 1.1 Gy. For the 328 precise in targeting, can result in dose spread to the 317 Ipsilateral lung, the highest D_{mean} was 11.0 Gy found 329 contralateral side. The heart was one of the critical

organs that required special attention. The IMRT technique showed the highest D_{mean} of 14.4 Gy (MC Log), beyond VMAT (6.9 Gy) and 3DCRT (1.3 Gy, TPS). The low dose volume distribution (V_5) reached 100 % in IMRT. The VMAT technique provides better protection to the heart with a more limited dose distribution. The highest maximum dose (D_1) to the spinal cord was recorded by IMRT at 10.7 Gy (MC Log). In contrast, the 3DCRT technique with TPS showed the lowest D_1 at 0.3 Gy, indicating the ability of this technique to protect the spinal cord from high-dose exposure. In addition, we evaluate the gamma index between MC-TPS and MC Log-TPS. The global GPR with 3%/3mm criteria and 10 % dose threshold is shown in Table 4.

346
347
348
349

Table 4. Global gamma pass rate of Monte Carlo and treatment plan.

Technique	GPR (%)	
	MC-TPS	MC Log-TPS
3DCRT	99.67	99.69
IMRT	99.98	99.50
VMAT	99.91	66.86

350
351

DISCUSSION

This study uses Monte Carlo PRIMO based software that allows modeling of 6 MV photon beam linac. Simulations performed in the first PRIMO segment will produce PSF containing information on energy, direction, angle, and particles under the chamber monitor. This PSF is then used for simulations in the next segment. This file will be validated to match the output of the linac used at MRCCC Siloam Semanggi Hospital.

The area at each point on the PDD along the central beam axis after d_{max} having a deviation tolerance limit of 2 %. While the build-up area is a high dose gradient area, a shift in position can cause a significant change in dose, therefore, the tolerance limit is prioritized at 2 mm [13]. In each area δ_1 and δ_2 has a confidence limit value that is still within the tolerance limit. For a field size of 10×10 cm², the value δ_1 is 2.2 %, while the value δ_2 is 0.3 mm. This causes the average deviation value to be larger and the standard deviation to be high [13]. Therefore, the confidence limit value exceeds the specified limit.

This area is an area within the beam field size but outside the central beam axis which is a high dose area and a small dose gradient. In Table 2 are obtained using Eqs. (3) and (4). By looking at the comparison between the results of the planning reconstruction simulation, sometimes the HI value in IMRT has more satisfactory results than VMAT. This shows that the dose coverage in both techniques does not have a definite difference, and none is superior to the other [13,14]. Different results are obtained when we compare the results of the dynalog file reconstruction simulation, HI in VMAT shows more satisfactory results than HI in IMRT in all patients. The HI value from the planning reconstruction simulation with the dynalog file in IMRT has a significant difference. In Table 3 the results of the dynalog file reconstruction are always greater than the planning. This difference is not found in VMAT, the difference between the results of the planning reconstruction and the dynalog file does not have a significant difference. These results agreed with Qodarul et al (2025) that VMAT had more satisfactory results than the HI value of IMRT [15]

The low CI value of the VMAT technique for the CI parameter (0.7) may be due to the complexity of dose planning for this technique. VMAT allows for more conformal dose distribution but also increases the risk of uncertainty in planning. The low HI value of the IMRT technique shows the superiority of this technique in producing a more uniform dose distribution on tumor targets. This is very important to minimize damage to the healthy tissue around the tumor. The small difference in CI values between 3D CRT and IMRT suggests that IMRT does not necessarily provide a significant advantage in terms of dose accuracy for CI parameters. However, the main advantage of IMRT lies in its ability to produce more conformal dose distributions. Meanwhile, in Table 3, the low dose volume parameter (V_5) also showed a significant difference, with IMRT (58.4 %, MC Log) showing a wider dose distribution than 3DCRT (3.3 %, TPS). This difference indicates that IMRT has a wider dose spread, which may increase the risk of lung toxicity.

The dose volume distribution confirms that the VMAT technique excels in balancing target coverage and OAR protection. In other words, VMAT provided more uniform dose coverage to the target while minimizing the dose to the OARs, particularly to the ipsilateral and contralateral lungs. However, the IMRT technique shows some weaknesses, especially in parameters such as D_{mean} and V_5 for heart and lung. This indicates a potential increase in the risk of toxicity that requires close monitoring. Meanwhile, 3DCRT has advantages in OAR protection but has shortcomings in target coverage, especially in dose homogeneity and conformity.

Almost all of the studies reported a GPR (Gamma Passing Rate) higher than 95 %. However, for the VMAT log, the GPR dropped significantly to

438 66.86 %. This indicates a substantial difference in
439 dose distribution between Monte Carlo (MC)
440 calculations using dynalog input and the Treatment
441 Planning System (TPS). This result is consistent
442 with the dosimetry values shown in Tables 2 and 4,
443 where VMAT demonstrated the lowest quality in
444 terms of Homogeneity Index (HI) and Conformity
445 Index (CI). Azzi et al. (2023) and Qodarul et al.
446 (2025) suggested that dose verification based on
447 linac log files should take into account the data
448 stream frequency and the limitations of the
449 software's internal processing [7,15].

450

451

452 CONCLUSION

453 This study found the 3DCRT showing superior
454 HI, CI, and OAR sparing compared to IMRT and
455 VMAT when the Linac log file was implemented.
456 However, since real patient anatomy varies, technique
457 selection should be personalized, balancing these
458 parameters. IMRT and VMAT displayed discrepancies
459 between TPS and Monte Carlo-simulated Linac log
460 data, suggesting issues in data transfer that require
461 further investigation.

462

463

464 ACKNOWLEDGMENT

465 The Author(s) wishes to thank Prof. Djarwani,
466 who has always provided moral support since the
467 beginning of this journey.

468

469

470 AUTHOR CONTRIBUTION

471 Rendra Dandi Sugandi and Akbar Azzi
472 equally contributed to this paper as the main authors.
473 Muhammad Fadli contributed to data collection.
474 Dwi Seno Kuncoro Sihono agreed and approved the
475 final version of the paper.

508

509

510

511

512

513

514

515

516

517

518 Notes:

519

520 • Please add 1 or more references citing
521 the Indonesian Atomic Journal, along
522 with the sentences that cite them.
523 (<https://atomindonesia.brin.go.id/index.php/aij>)

REFERENCES

- 476 1. M. Rodriguez and L. Brualla, Radiati. Oncol.
477 14 (2019) 67.
- 478 2. S. B. Lim, P. G. Sripes, M. Napolitano *et al.*,
479 J. Appl. Clin. Med. Phys. 22 (2021) 183.
- 480 3. M. Miften, A. Olch, D. Mihailidis *et al.*,
481 Med. Phys. 45 (2018) e53.
- 482 4. A. Altuwayrish, M. Ghorbani, M. Bakhshandeh
483 *et al.*, Rep. Pract. Oncol. Radiother. 27
484 (2022) 863.
- 485 5. H. Aamri, A. Fielding, A. Aamry *et al.*, Radiat.
486 Phys. Chem. 178 (2021) 109013.
- 487 6. E. E. Klein, J. Hanley, J. Bayouth *et al.*,
488 Med. Phys. 36 (2009) 4197.
- 489 7. A. Azzi, G. Heilemann, D. Georg *et al.*,
490 Z. Med. Phys. 35 (2025) 152.
- 491 8. J. R. Kerns, N. Childress, and S. F. Kry, Radiat.
492 Oncol. 9 (2014) 1.
- 493 9. A. W. Lee, W. T. Ng, J. J. Pan *et al.*, Int. J.
494 Radiation Oncol. Biol. Phys. 105 (2019) 567.
- 495 10. H. G. Menzel, J. ICRU 10 (2010) Report 83.
- 496 11. A. V. Riet, A. C. A. Mak, M. A. Moerlan *et al.*,
497 Int. J. Radiation Oncol. Biol. Phys. 37
498 (1997) 731.
- 499 12. D. A. Low, W. B. Harms, S. Mutic *et al.*,
500 Med. Phys. 25 (1998) 656.
- 501 13. J. Venselaar, H. Welleweerd, and B. Mijnheer,
502 Radiother. Oncol. 60 (2001) 191.
- 503 14. Z. Ouyang, Z. Liu Shen, E. Murray *et al.*,
504 J. Appl. Clin. Med. Phys. 20 (2019) 39.
- 505 15. M. R. F. Qodarul, D. Ryangga, A. D. Handika,
506 *et al.*, Radiat. Phys. Chem. 235 (2025) 112825.
507